

# CRes User Guide

LEIGHTON M. WATSON  
Stanford University  
leightonwatson@stanford.edu

March 29, 2019

## I. INTRODUCTION

**CRes** (Crater Resonance) is a one-dimensional (1D) numerical method for solving the linear acoustic wave equation within a volcanic crater. For a specified crater geometry and excitation source at the base of the crater, **CRes** computes the velocity and pressure at the crater outlet and can propagate the signal to an infrasound receiver some distance from the outlet. The linear acoustic wave equation is written in terms of two first-order differential equations for pressure and acoustic flow and is solved by **CRes** using a finite-difference frequency-domain method. **CRes** is written in MATLAB and runs efficiently on a standard desktop/laptop computer. For more details and examples of the application of **CRes** see:

- Watson, L. M., Dunham, E. M., and Johnson, J. B. Simulation and inversion of harmonic infrasound from open-vent volcanoes using an efficient quasi-1D crater model, *Journal of Volcanology and Geothermal Research*, submitted 28 Dec 2018, revised 19 Mar 2019.
- Johnson, J. B., Watson, L. M., Palma, J. L., Dunham, E. M., and Anderson, J. F. (2018) Forecasting the eruption of an open-vent volcano using resonant infrasound tones, *Geophysical Research Letters*, 45, <https://doi.org/10.1002/2017GL076506>.

## II. DIRECTORY

- **demo** - script files for demonstration
  - `exampleX.m` - example script files
  - `Johnson2018.mat` - example crater geometry from Johnson et al. (2018)
  - `Richardson2014.mat` - example crater geometry from Richardson et al. (2014)
- **doc** - documentation including user guide and license file
- **source/SBPoperators** - function files associated with numerical implementation
- **source/resonance** - function files for **CRes**
  - `resonance1d.m` - main code
  - `problemParameters` - specifies model parameters
  - `pressurePerturbation.m` - computes pressure perturbation (infrasound signal) at a distance away from the crater
  - `flanged_opening.m` - treatment of open end of crater
  - `resPeakProps.m` - computes resonant frequency and quality factor of spectral peaks
  - `sourceFunction.m` - specifies source function (Gaussian or Brune)

**CRes** is freely available online at <https://github.com/leighton-watson/CRes> and is distributed under the MIT license (see `license.txt` for details).

### III. MODEL DESCRIPTION

Here, I provide an overview of **CRes**. For more details see Watson et al., (2019). **CRes** assumes linear wave propagation, which enables the infrasound signal,  $\Delta p$ , observed at a distance,  $r$ , from the crater outlet to be written as:

$$\Delta p(t, r) = T(t, r) * s(t) \quad (1)$$

where  $T$  is the acoustic response function, which depends on the crater and atmospheric properties, that describes the theoretical infrasound signal generated by an impulsive excitation at the base of the crater, and  $s(t)$  is the finite-duration source at the base of the crater. The source expressed as a volumetric flow rate of air within the crater being push upwards, or pulled downwards, by the source process ( $\text{m}^3/\text{s}$ ). **CRes** is written in the frequency domain where the time-domain convolution is replaced by multiplication:

$$\Delta p(\omega, r) = T(\omega, r)s(\omega), \quad (2)$$

where  $\omega$  is the angular frequency.

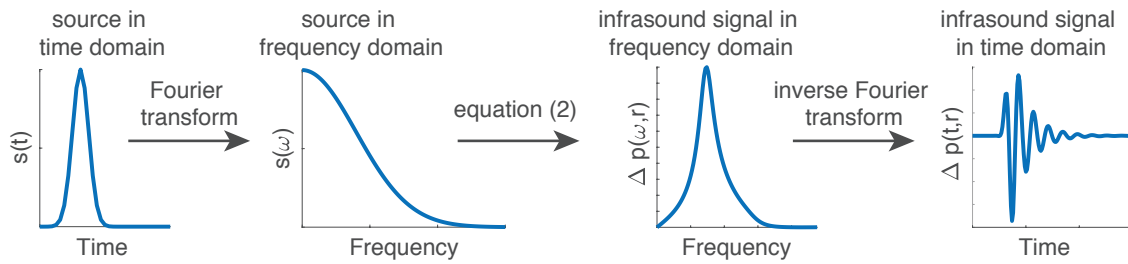


**Figure 1:** The modeling workflow is to start with a specified source function,  $s(t)$ , and take the Fourier transform to get  $s(\omega)$ . The infrasound signal in the frequency domain,  $\Delta p(\omega, r)$ , is calculated by equation 2 and the inverse Fourier transform is used to obtain the infrasound signal in the time domain,  $\Delta p(t, r)$ .

The acoustic response function,  $T$ , is divided into 1.) the crater acoustic response function,  $C$ , which describes wave propagation and resonant modes inside the volcanic crater, and 2.) the atmospheric response function,  $P$ , which describes acoustic radiation from the crater to the infrasound station. The crater acoustic response,  $C$ , is defined as

$$C(\omega) = \frac{U(\omega, 0)}{s(\omega)}, \quad (3)$$

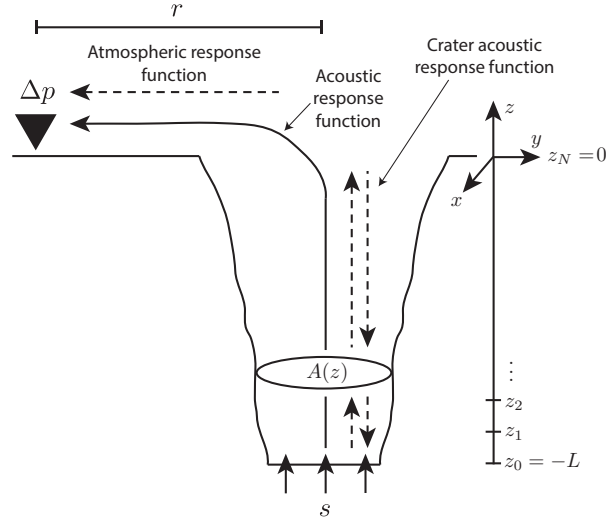
where  $U$  is the volumetric flow rate associated with acoustic waves ( $U = vA$  is the acoustic flow where  $A$  is the cross-sectional area, which can vary as a function of depth, and  $v$  is the vertical particle velocity). The atmosphere response function,  $P$ , is defined as

$$P(\omega, r) = \frac{\Delta p(\omega, r)}{U(\omega, 0)}, \quad (4)$$

allowing the acoustic response function,  $T$ , to be expressed as

$$T(\omega, r) = C(\omega)P(\omega, r) = \frac{U(\omega, 0)}{s(\omega)} \frac{\Delta p(\omega, r)}{U(\omega, 0)} = \frac{\Delta p(\omega, r)}{s(\omega)}. \quad (5)$$

**Figure 2:** Schematic of model. The infrasound signal,  $\Delta p$ , observed at a distance  $r$  from the crater is related to the excitation source at the base of the crater,  $s$ , by the acoustic response function,  $T$ , which includes the crater acoustic response function that describes wave propagation inside the crater and associated resonant modes, and the atmosphere response function, which describes acoustic radiation from the crater outlet to the receiver.



### i. Crater Acoustic Response Function

This section describes how to calculate the crater acoustic response function,  $C$ . The crater is modeled as quasi-one-dimensional (allowing for changes in cross-sectional area with depth) and axisymmetric. Acoustic waves inside the crater are described by linear acoustics written as a system of first-order partial differential equations:

$$\frac{\partial U}{\partial t} + \frac{A}{\rho} \frac{\partial p}{\partial z} = 0, \quad (6)$$

$$\frac{\partial p}{\partial t} + \frac{K}{A} \frac{\partial U}{\partial z} = 0, \quad (7)$$

where  $p$  is the pressure. The air inside the crater is described as an ideal gas with ambient density,  $\rho$ , and fluid bulk modulus,  $K$ , which is proportional to the ambient pressure for an ideal gas. Density and pressure are related by the ideal gas equation of state:

$$p = \rho RT, \quad (8)$$

where  $R$  is the specific gas constant and  $T$  is the temperature, not to be confused with response function  $T$  in equations (1) and (2). The speed of sound is

$$c = \sqrt{\gamma RT}, \quad (9)$$

where  $\gamma$  is the ratio of specific heats ( $\gamma = 1.4$  for diatomic gases such as air).

The governing equations are solved in the frequency domain and can be written as a system of first-order ordinary differential equations:

$$i\omega U + \frac{A}{\rho} \frac{\partial p}{\partial z} = 0, \quad (10)$$

$$i\omega p + \frac{K}{A} \frac{\partial U}{\partial z} = 0. \quad (11)$$

The model requires two boundary conditions, one at the bottom of the crater and one at the crater outlet. At the bottom,  $z = -L$ , of the crater the acoustic flow is specified as the source-time

function:

$$U(t, -L) = s(t) = \iint_{A(L)} v(x, y, t) dx dy. \quad (12)$$

At the crater outlet,  $z = 0$ , the pressure and acoustic flow are related by the terminating impedance,  $Z_T$  (Rossing and Fletcher, 2004):

$$\frac{p(\omega, 0)}{U(\omega, 0)} = Z_T(\omega). \quad (13)$$

A constant pressure boundary condition could be applied at the outlet. However, this results in perfect reflection of acoustic waves. In order to allow acoustic waves to escape into the atmosphere and be recorded as infrasound, a more accurate description of the outlet is required. Here, a flanged opening is assumed (Olson, 1957; Kinsler et al., 2000; Rossing and Fletcher, 2004) and the terminating impedance is given by (Rossing and Fletcher, 2004)

$$Z_T = R + iX, \quad (14)$$

where  $i$  indicates the imaginary unit,  $R$  is the acoustic resistance

$$R = Z_a \left[ \frac{(ka)^2}{2} - \frac{(ka)^4}{2^2 \cdot 3} + \frac{(ka)^6}{2^2 \cdot 3^2 \cdot 4} - \dots \right], \quad (15)$$

and  $X$  is the acoustic reactance

$$X = \frac{Z_a}{\pi(ka)^2} \left[ \frac{(2ka)^3}{3} - \frac{(2ka)^5}{3^2 \cdot 5} + \frac{(2ka)^7}{3^2 \cdot 5^2 \cdot 7} - \dots \right], \quad (16)$$

with  $k$  the wavenumber,  $a$  the crater radius at the outlet and  $Z_a = \rho_a c_a / A(0)$  where  $\rho_a$  and  $c_a$  are the density and speed of sound in the atmosphere, respectively, and  $A(0)$  is the cross-sectional area of the crater outlet.

## ii. Atmosphere Response Function

This section describes how to calculate the atmosphere response function,  $P$ . Propagation of the infrasound signal from the crater outlet to the receiver is described as axisymmetric radiation from a baffled piston embedded in an infinite plane (Rossing and Fletcher, 2004):

$$\Delta p(\omega, r) = i\omega \exp(-ikr) \frac{\rho_a a^2}{2r} \left[ \frac{2J_1(ka \sin \theta)}{ka \sin \theta} \right] \frac{U(\omega, 0)}{\pi a^2}, \quad (17)$$

where  $J_1$  is a Bessel function of order one,  $\theta$  is the angle between the negative  $z$ -axis and the receiver (e.g.,  $\theta = \pi/2$  for a receiver located on the plane perpendicular to crater orientation),  $\rho_a$  is the density of the atmosphere, and  $a$  is the crater radius at the outlet. The baffled piston model reduces to the monopole source description (e.g., Woulff and McGetchin, 1976; Johnson and Miller, 2014) for radiation in a half-space in the low frequency limit when  $ka \ll 1$ ,

$$\Delta p(\omega, r) = i\omega \exp(-ikr) \frac{\rho_a a^2}{2r} \frac{U(\omega, 0)}{\pi a^2}. \quad (18)$$

## IV. NUMERICAL IMPLEMENTATION

Equations 10 and 11 are solved using a summation-by-parts finite-difference discretization scheme (Del Rey Fernández et al., 2014; Svärd and Nordström, 2014), which is discussed in this section.

The domain  $(-L \leq z \leq 0)$  is discretized into  $N + 1$  evenly spaced grid points,  $z_i$ ,  $i = 0, 1, 2, \dots, N$  where  $z_0 = -L$  is at the base of the crater where the source is located and  $z_N = 0$  is at the top of the crater. A field such as  $p(z, t)$  is approximated at the grid points with the grid values stored in a vector  $\mathbf{p}(t)$  with components  $p_i(t) \approx p(z_i, t)$ . The spatial derivatives are approximated using a summation-by-parts (SBP) differentiation matrix,  $\mathbf{D}$ , such that the vector  $\mathbf{D}\mathbf{p}$  contains approximations to  $\partial p / \partial z$  at the grid points (Karlstrom and Dunham, 2016). The discrete equations are

$$i\omega \mathbf{U} + \frac{A}{\rho_{\text{amb}}} \mathbf{D}\mathbf{p} = -\theta_1(U_0 - \hat{U}_0)\mathbf{e}_0 - \theta_2(U_N - \hat{U}_N)\mathbf{e}_N, \quad (19)$$

$$i\omega \mathbf{p} + \frac{K}{A} \mathbf{D}\mathbf{U} = -\theta_3(p_0 - \hat{p}_0)\mathbf{e}_0 - \theta_4(p_N - \hat{p}_N)\mathbf{e}_N, \quad (20)$$

where the terms on the right are the implementation of the boundary conditions in the SAT framework. Scalars  $\theta_1 - \theta_4$  are penalty parameters that are chosen to ensure a stable numerical discretization (Kozdon et al., 2012):

$$\theta_1 = \theta_3 = \frac{c}{H_{00}}, \quad (21)$$

$$\theta_2 = \theta_4 = \frac{c}{H_{NN}}, \quad (22)$$

where  $\mathbf{H}$  is a symmetric positive definite matrix such that  $\mathbf{D} = \mathbf{H}^{-1}\mathbf{Q}$  where  $\mathbf{Q}$  is an almost skew symmetric matrix with the property that  $\mathbf{Q}^T + \mathbf{Q} = \text{diag}[-1 \ 0 \ \dots \ 0 \ 1]$  (Karlstrom and Dunham, 2016).

The variables with a circumflex,  $\hat{U}_0, \hat{U}_N, \hat{p}_0, \hat{p}_N$ , are the target values for acoustic flow and pressure at the boundary points while  $U_0, U_N, p_0$  and  $p_N$  are the known grid values. The target values are chosen to satisfy the desired boundary conditions exactly while preserving the characteristic variable carrying information from the interior of the domain to the boundary. The vectors  $\mathbf{e}_0 = [1 \ 0 \ \dots \ 0]^T$  and  $\mathbf{e}_N = [0 \ \dots \ 0 \ 1]^T$  isolate the effect of the penalty terms to the boundary points (Karlstrom and Dunham, 2016).

The characteristic variables that carry information from the interior of the domain to the boundaries are

$$p_0 - Z_0 U_0 = \hat{p}_0 - Z_0 \hat{U}_0, \quad (23)$$

$$p_N + Z_N U_N = \hat{p}_N + Z_N \hat{U}_N, \quad (24)$$

where  $Z = \rho c / A$  is the acoustic impedance. The acoustic flow is specified at the base of the crater ( $\hat{U}_0$  is known; equation 12) and hence equation 23 can be rearranged to give

$$\hat{p}_0 = p_0 + Z_0(\hat{U}_0 - U_0). \quad (25)$$

At the crater outlet, the pressure is related to the acoustic flow by the terminating impedance,  $Z_T$ :

$$\hat{p}_N = Z_T \hat{U}_N. \quad (26)$$

The terminating impedance is calculated using a flanged opening approximation (equation 14; Kinsler et al., 2000; Rossing and Fletcher, 2004). Substituting equation 26 into equation 24 gives the outlet boundary conditions:

$$\hat{U}_N = \frac{p_N + Z_N U_N}{Z_T + Z_N}, \quad (27)$$

$$\hat{p}_N = Z_T \left( \frac{p_N + Z_N U_N}{Z_T + Z_N} \right). \quad (28)$$

## V. USING CRes

This section covers the workflow of using **CRes**, which is outlined below, and shows how to use **CRes** to calculate the infrasound signal generated by acoustic resonance of a volcanic crater.

1. Define model properties and geometry
2. Compute acoustic response function,  $T$
3. Specify source function
4. Compute infrasound signal

### i. Define model properties and geometry

The first step is to define the properties of the air within the crater and the atmosphere by calling the function `problemParameters.m`.

```
M = problemParameters(); % load parameter values from problemParameters.m
```

This function accepts no inputs and outputs a structure `M` that contains the properties (density, temperature, pressure etc.) of the air in the crater and the atmosphere. Also defined in `problemParameters.m` is the distance from the crater outlet to where the infrasound signal is calculated. A future release will enable the function to accept input property values. Until then, parameters are specified in the function file. **CRes** allows for properties (density, temperature) to be different within the crater and atmosphere but assumes properties are constant.

The next step is to specify the crater geometry as a matrix with two columns. The first column is the depth (at equally spaced intervals) and the second column is the corresponding radius. The matrix must be arranged so that the depths monotonically decrease starting from the largest value. For the examples included here the crater geometry is from Johnson et al. (2018) and saved as `Johnson2018.mat`, which can be loaded and formatted by the following code:

```
load('Johnson2018'); % load geometry
shape = flipud(geometry); % reformat geometry matrix to be read by solver
```

The geometry can be specified in alternative ways (e.g., read from a text file) provided the information is passed to the solver in the format shown in Figure 3.

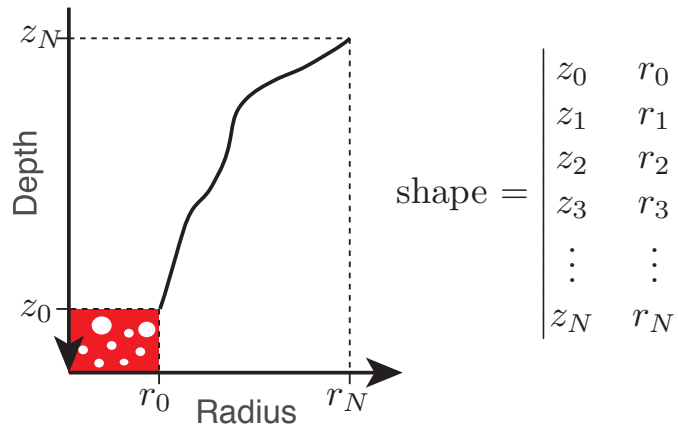


Figure 3: Format of two-column matrix containing geometry information.

## ii. Compute acoustic response function, $T$

The bulk of the computational expense is calculating the acoustic response function,  $T$ . This is done by `resonance1d.m`, which computes both the crater acoustic response function,  $C$ , and the atmosphere response function,  $P$ .

```
function output = resonance1d(geometry, depth, freq, Nf, style, order, M)
% computes the acoustic response function for an axisymmetric crater
```

| Inputs:         | Description  | Default Value            |
|-----------------|--|--------------------------|
| geometry        | $(N + 1) \times 2$ matrix containing geometry  | Required                 |
| depth           | Maximum crater depth, $z_0$  | Required                 |
| freq            | Minimum and maximum frequencies  | Required                 |
| Nf              | Number of frequency samples  | Nf = 100                 |
| style           | Order of numerical scheme (4, 6, or 8)   | order = 8                |
| order           | Model of atmospheric radiation ('baffled piston' or 'monopole')                        | style = 'baffled piston' |
| M               | Structure containing model parameters  | M = problemParameters()  |
| Outputs:        | Description  | Dimension                |
| output.geometry | Matrix containing geometry   | $(N + 1) \times 2$       |
| output.depth    | Maximum crater depth   | 1                        |
| output.f        | Frequency vector with Nf entries   | $1 \times Nf$            |
| output.T        | Transfer function for pressure and acoustic flow at crater depth positions in geometry | $2(N + 1) \times Nf$     |
| output.pOutlet  | Transfer function for outlet pressure  | $1 \times Nf$            |
| output.vOutlet  | Transfer function for outlet velocity  | $1 \times Nf$            |
| output.P        | Transfer function for pressure at distance $r$ from crater outlet                      | $1 \times Nf$            |

**Table 1:** Inputs and outputs of `resonance1d.m`. Transfer functions map an impulsive excitation (expressed as volumetric flow rate) at the base of crater to the listed quantity.

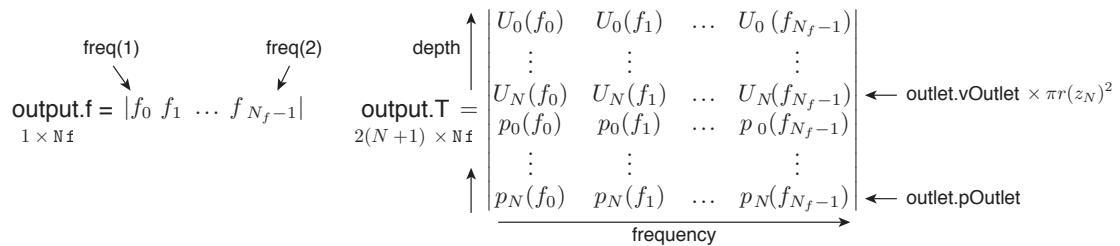


**Figure 4:** Format outputs from `resonance1d.m`.

The function `flanged_opening.m` is used to calculate the terminating impedance (equation 14) while `pressurePerturbation.m` is used to compute the atmosphere response function. There are two possible models of the atmospheric radiation: baffled piston (equation 17) and monopole (equation 18).

### iii. Specify source function

In **CRes**, acoustic waves are excited by a source at the base of the crater, which is expressed as a volumetric flow rate of air within the crater being pushed upwards, or pulled downwards, by the source process ( $\text{m}^3/\text{s}$ ). The source can be specified by `sourceFunction.m`, which allows for either a Gaussian or Brune function (Brune, 1970).

```
function [S, f, s, t] = sourceFunction(A, L, srcStyle, resParams)
% computes source function in (s) time and (S) frequency domains
```

| Inputs:   | Description  |
|-----------|--|
| A         | Source amplitude   |
| L         | Source width   |
| srcStyle  | Functional form of source 'Gauss' or 'Brune'   |
| resParams | Parameters to ensure source description is consistent with transfer function<br>resParams = [T N]<br>T = total time, N = number of grid points |
| Outputs:  | Description  |
| S         | Source in frequency domain   |
| f         | Frequency  |
| s         | Source in time domain  |
| t         | Time   |

**Table 2:** Inputs and outputs of `sourceFunction.m`.

Alternative source functions or user defined source data can also be used by **CRes** provided the source is discretized in the same way as the transfer function.

### iv. Compute infrasound signal

Once the transfer function from the volumetric flow rate at the base of the crater to the receiver, `output.P`, and the source function in the frequency domain, `S`, have been calculated, it is straightforward to compute the infrasound signal by multiplying the source with the transfer function in the frequency domain (equation 2):

```
dP = output.P .* S(1:N/2+1);
```

where `dP` is the excess pressure in the frequency domain. Note that the transfer function is only specified at positive frequencies so only the positive frequencies from the source (`1:N/2+1`) are used in the multiplication. The inverse Fourier transform can be used to convert the signal back to the time domain:

```
dP_pos = dP(1:N/2+1);
dP_full = [dP_pos conj(dP_pos(end-1:-1:2))]; % reflect about f = 0. Take complex
        conjugate for negative frequencies
dP_full(N/2+1) = real(dP_full(N/2+1)); % entry at Nyquist must be real
dP_time = ifft(dP_full, 'symmetric')/dt; % inverse fourier transform
```

The resonant frequency, `f0`, and quality factor, `Q`, of the infrasound signal can be computed using `resPeakProps.m`.

```
[f0,Q] = resPeakProps(output.f,dP);
```



## VI. EXAMPLES

For demonstration purposes, two example script files are included that simulate crater acoustic resonance at Villarrica volcano. `example1.m` computes the resonant modes of Villarrica's crater for a single depth while `example2.m` shows how to compute the resonant frequency and quality factor as a function of the position of the lava lake within the crater. The crater geometry has been previously calculated from visual observations using structure-from-motion (Johnson et al., 2018) and is saved as `Johnson2018.mat`.

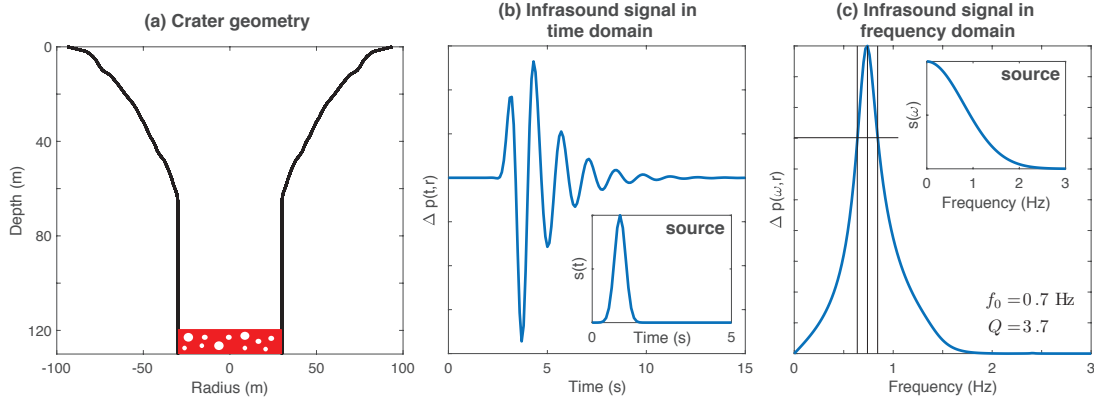


**Figure 5:** Outputs from `example1.m` showing (a) crater geometry with lava lake at 120 m below the crater rim, (b) infrasound signal in the time domain and (c) in the frequency domain. Insets show the source (volumetric flow rate at base of crater/surface of lava lake).

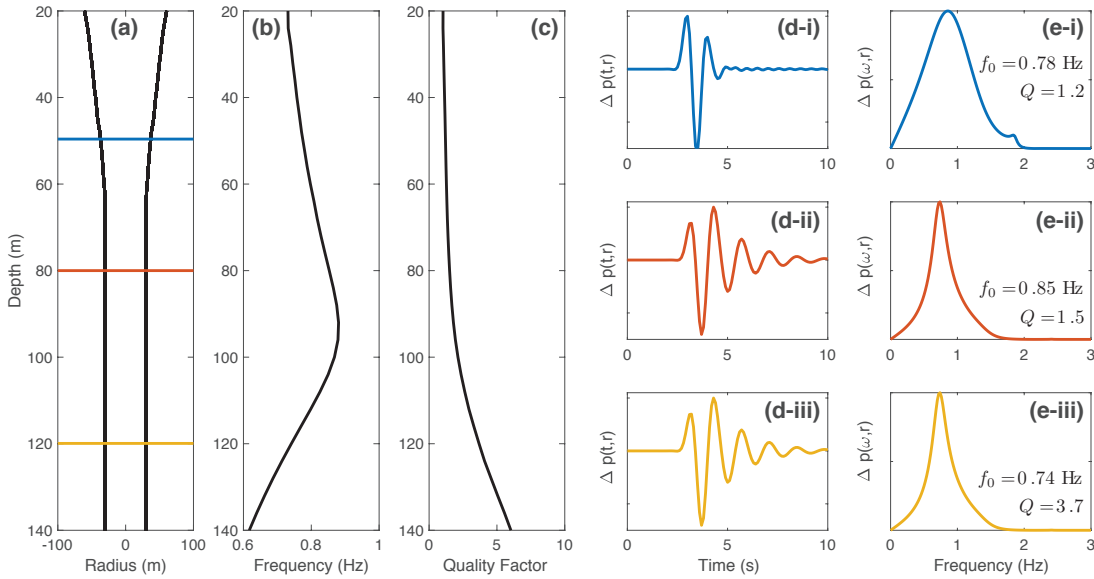


**Figure 6:** Outputs from `example2.m` showing simulated infrasound signal as a function of depth. (a) Crater geometry, (b) Resonant frequency and (c) quality factor as a function of depth. Infrasound signal in the (d) time and (e) frequency domains for crater depths of (i) 50 m, (ii) 80 m, and (iii) 120 m. Acoustic waves are excited by a Gaussian pulse with  $\sigma = 0.2$  s, the same source as for `example1.m`.

## REFERENCES

- Brune, J. N., 1970. Tectonic stress and the spectra of seismic shear waves from earthquakes. *Journal of Geophysical Research* 75 (26), 4997–5009.
- Del Rey Fernández, D. C., Hicken, J. E., Zingg, D. W., 2014. Review of summation-by-parts operators with simultaneous approximation terms for the numerical solution of partial differential equations. *Computers and Fluids* 95, 171–196.
- Johnson, J. B., Miller, A. J. C., 2014. Application of the Monopole Source to Quantify Explosive Flux during Vulcanian Explosions at Sakurajima Volcano (Japan). *Seismological Research Letters* 85 (6).
- Johnson, J. B., Watson, L. M., Palma, J. L., Dunham, E. M., Anderson, J. F., 2018. Forecasting the eruption of an open-vent volcano using resonant infrasound tones. *Geophysical Research Letters*, 1–8.
- Karlstrom, L., Dunham, E. M., 2016. Excitation and resonance of acoustic-gravity waves in a column of stratified, bubbly magma. *Journal of Fluid Mechanics* 797, 431–470.
- Kim, K., Lees, J. M., 2011. Finite-difference time-domain modeling of transient infrasonic wavefields excited by volcanic explosions. *Geophysical Research Letters* 38 (6), 2–6.
- Kinsler, L. E., Frey, A. R., Coppens, A. B., Sanders, J. V., 2000. *Fundamentals of Acoustics*, 4th Edition. John Wiley and Sons, New York.
- Kozdon, J. E., Dunham, E. M., Nordström, J., 2012. Interaction of waves with frictional interfaces using summation-by-parts difference operators: Weak enforcement of nonlinear boundary conditions. *Journal of Scientific Computing* 50 (2), 341–367.
- Olson, H. F., 1957. *Acoustical engineering*. Van Nostrand Company, Princeton, New Jersey.
- Richardson, J. P., Waite, G. P., Palma, J. L., 2014. Varying seismic-acoustic properties of the fluctuating lava lake at Villarrica volcano, Chile. *Journal of Geophysical Research: Solid Earth*, 1–14.
- Rossing, T. D., Fletcher, N. H., 2004. *Principles of Vibration and Sound*, 2nd Edition. Vol. 1. Springer.
- Svärd, M., Nordström, J., 2014. Review of summation-by-parts schemes for initial-boundary-value problems. *Journal of Computational Physics* 268, 17–38.
- Woulff, G., McGetchin, T. R., 1976. *Acoustic noise from volcanoes - Theory and experiment*.